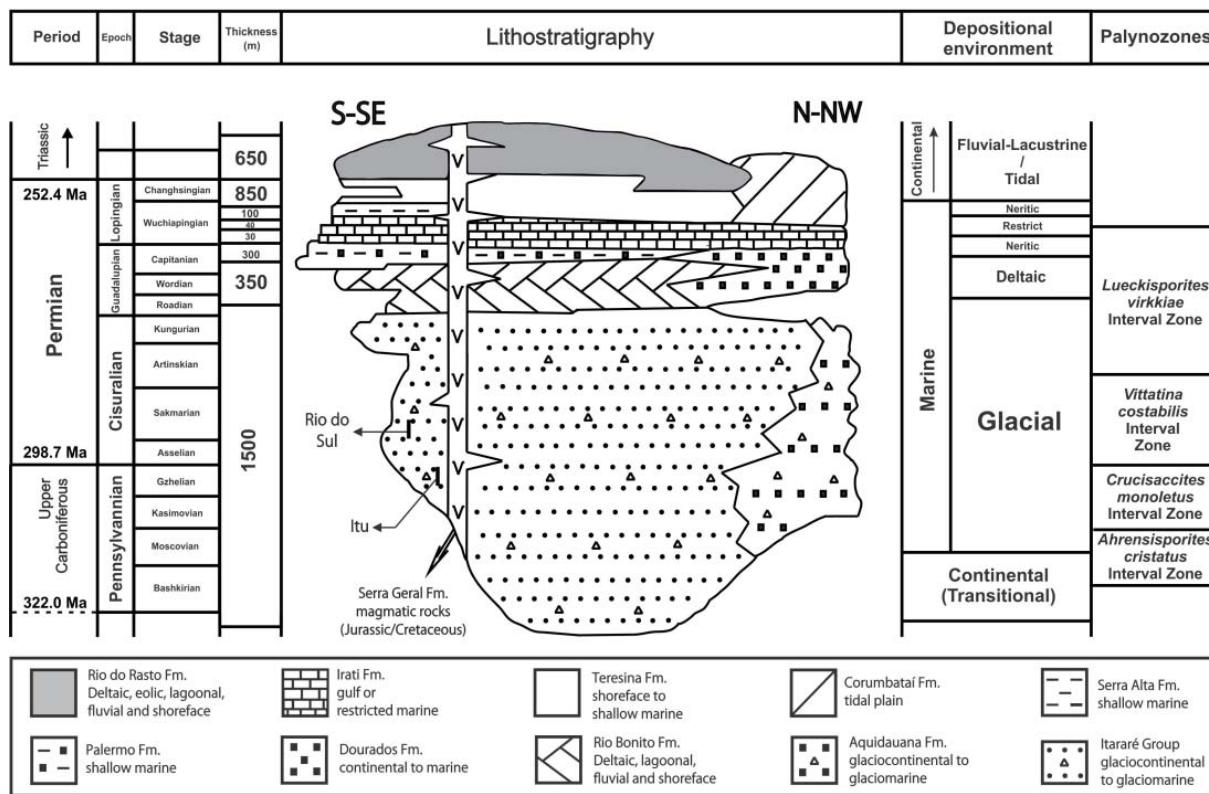


## GSA DATA REPOSITORY 2012009

### Franco, D.R., Hinnov, L.A., Ernesto, M., Millennium-Scale Climate Cycles in Permian-Scale Climate Cycles in Permian-Carboniferous Rhythmites: Permanent Feature Throughout Geologic Time?

#### A. Geological Setting

The Itararé Group (IG) of the Paraná Basin, Brazil includes one of the thickest sequences of Gondwana Paleozoic glacial sediments in the world (about 1300 m), covering about 20 to 40 Ma from Middle-Late Carboniferous to Early Permian (Santos *et al.*, 1996). Although the areal extent of the Paraná sedimentary basin is large ( $1.6 \times 10^6 \text{ km}^2$ ; Fig. 1) outcrops are confined to narrow strips on the eastern and northwestern borders due to thick magmatic cover from the Early Cretaceous Serra Geral Formation. In the central portion of the basin, the IG is subdivided into Lagoa Azul, Campo Mourão and Taciba formations, mainly constituted of sandstones and diamictites, with minor presence of massive or laminated mudstones (Eyles *et al.*, 1993). The lower part of the sequence comprises sediments of glacio-lacustrine origin; a gradual and stronger marine influence occurs upwards (Fig. DR1). Dominant facies correspond to subaqueous gravity flows, resulting in high sedimentation and steep, fault-bounded basin margins. These and other glaciotectonic features (e.g. roche moutonnée, striated surfaces, diamictites, regular rhythmites with dropstones) record an advance-retreat record of ice-masses originating from a large southern African ice sheet, along a NW-SE direction (Rocha-Campos, 1967; França & Potter, 1991; Eyles *et al.*, 1993; Santos *et al.*, 1996; Rocha-Campos *et al.*, 2000; Vesely & Assine, 2002; Archanjo *et al.*, 2006).



**Figure DR1.** Distribution of stratigraphic supersequences in the Paraná Basin, SE Brazil. The Itararé Group is classified as a Gondwana I Supersequence. Itu and Rio do Sul quarries are indicated. From Franco *et al.* (in press).

Two conspicuous exposures of rhythmites are located in the city of Itu (Itu quarry; São Paulo State) and near the city of Rio do Sul (Itaú quarry; Santa Catarina State), and are the subject of this study. The Itu (IT) quarry ( $23^{\circ} 16' S$ ;  $47^{\circ} 19' W$ ; Fig. DR2) constitutes one of the best-preserved exposures of rhythmites in the Paraná Basin (Rocha-Campos, 2000). It exposes > 28 m of 260 cm-scale couplets in a continuous sequence. Individual layers vary in thickness from 50 to 1.5 cm, thinning upward. The Rio do Sul (RS) rhythmites ( $27^{\circ} 10' S$ ;  $49^{\circ} 35' W$ ; Fig. DR3) consist of couplets varying from 1.2 cm – 32 cm, and thickening upward. In both sequences dropstones testify to a strong glacial influence, associated with a large meltwater input Santos *et al.* (1992). Eyles *et al.* (1993) interpreted a calm depositional setting; Canuto (1993) suggested sedimentation in a proximal glaciomarine depositional system. Field photos are available in Franco (2007) and Franco *et al.* (in press).

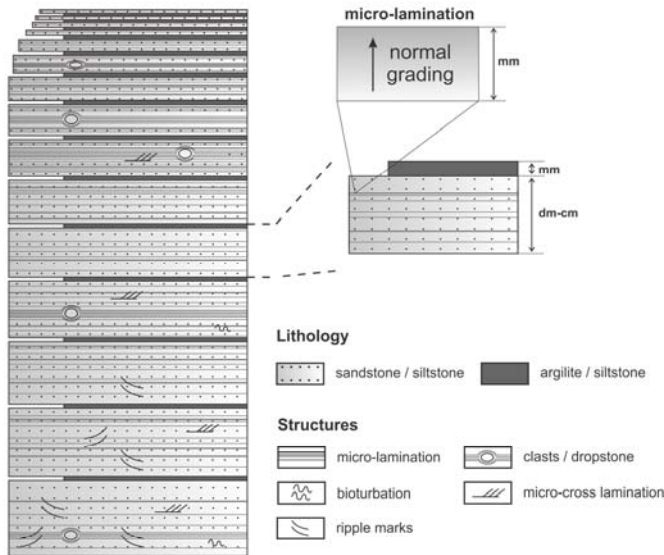


**Figure DR2.** Stratigraphy of the Itu rhythmites outcrop at Itu Quarry. Modified after Franco *et al.* (in press).

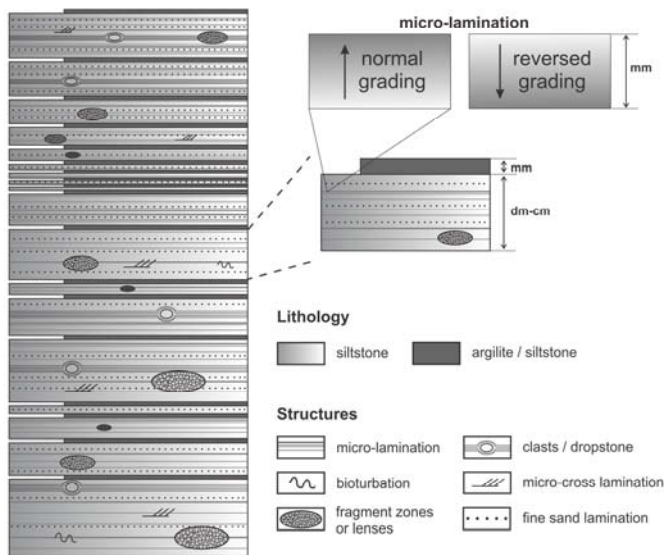


**Figure DR3.** Stratigraphy of the Rio do Sul rhythmites at Itau Quarry. Modified after Franco *et al.* (in press).

## B. Sampling preparation for high-resolution magnetostratigraphic data series

The oriented blocks used in this work (Fig. DR4) are essentially the same as those analyzed by Sinito *et al.* (1981) and Roch-Campos *et al.* (1981), collected from the IT and RS quarries. Block orientation was determined by magnetic and sun compasses, wherever possible. One block (Fig. DR4B) corresponds to a piece of a light sandy/silty layer topped by dark shale, and intercalated by thinner layers of dark shale. The preexisting sample collections (above) were not complete anymore, and additional sampling was performed in order to fill the gaps. However, due to the present quarry conditions, the former levels of the RS collection could not be identified, and some gaps still persist. We recovered blocks from 150 IT layers, and 94 from the RS rhythmites. From each block one inch-diameter cylinders were cut across the whole layer thickness (Figs. DR4B and DR4C); the cylinders were then sliced into 2.2 cm specimens from bottom to top; the uppermost specimen from each layer being generally smaller than the standard height. A total of 163 (IT) and 125 (RS) specimens were prepared for magnetic cleaning routines and bulk susceptibility ( $K_Z$ ) measurements (respectively conducted by the use of a 2G SQUID magnetometer housed in a low field room and a Minisep susceptometer (Molspin Ltd., UK)), which allowed us to build the magnetostratigraphic data series analyzed in this work (Fig. 2; Tables DR1 and DR2).

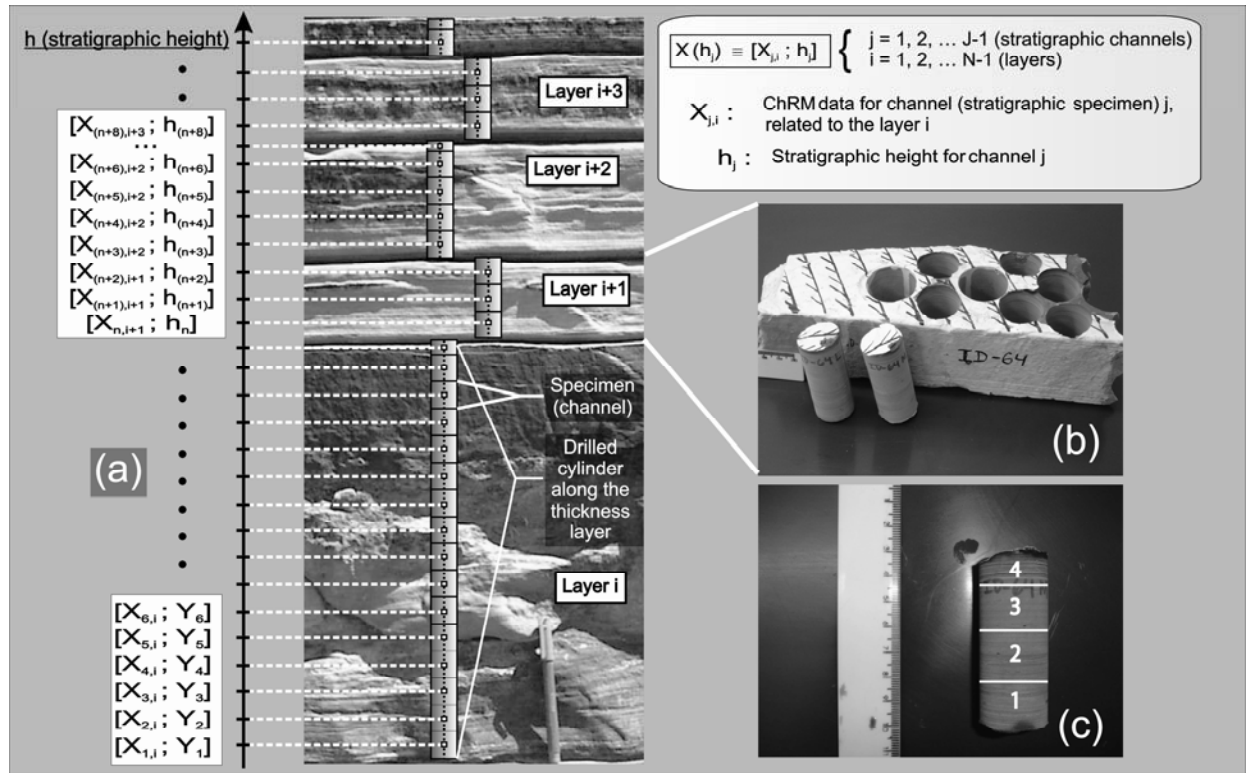


**Figure DR4:** (A) Sketch of sampling for acquisition of magnetostratigraphic data series. Declination/inclination of characteristic remanent magnetization ( $D_{\text{ChRM}}/I_{\text{ChRM}}$ ) and bulk susceptibility ( $K_Z$ ). (B) detail of an oriented block corresponding to a given lithological couplet and two inch-diameter cylinders which were cut crossing the whole block thickness; (C) detail of an inch-diameter cylinder and schematic sketched of 2.2 cm height specimens along its thickness. From Franco (2007).

### C. Paleomagnetic and K<sub>Z</sub> data

**Table DR1** –Paleomagnetic and bulk susceptibility (K<sub>Z</sub>) measurements of Permo-Carboniferous rhythmites from Itu (IT rhythmites), state of São Paulo, S. Brazil (47.26°W 23.17°S). From Franco (2007).

Site		Direction of ChRM		Bulk Susceptibility
Stratigraphic Position	Relative Height (mm)	Declination (°E)	Inclination (°)	K <sub>Z</sub> (10 <sup>-5</sup> CGS)
1	46.0	177.5	28.9	31.2
2	105.7	230.8	23.3	30.6
3	133.1	231.4	21.8	38.7
4	160.5	228.2	25.3	41.2
5	187.9	225.3	28.5	39.5
6	215.3	224.8	28.1	33.8
7	240.2	155.7	22.4	27.5
8	262.6	147.5	20.8	37.5
9	285.0	147.9	25.3	31.4
10	307.4	149.1	24.9	28.4
11	329.8	142.9	31.8	26.2
12	354.8	148.7	21.5	29.9
13	382.3	144.4	23.4	28.4
14	407.5	133.3	23.2	24.8
15	430.5	135.0	21.6	23.7
16	455.3	12.0	23.3	23.2
17	481.8	54.0	37.0	23.0
18	511.0	130.5	23.2	25.6
19	541.5	130.4	20.5	24.1
20	560.8	158.1	20.3	25.9
21	570.3	156.9	23.9	24.4
22	596.5	133.1	20.5	25.0
23	633.5	139.2	26.0	23.2
24	666.0	126.5	24.2	26.3
25	700.0	128.3	19.7	26.1
26	734.0	133.8	25.6	25.1
27	762.3	156.6	19.6	23.9
28	784.8	153.3	22.7	22.3
29	815.5	150.5	24.2	23.3
30	850.0	150.4	24.6	22.8
31	874.8	146.2	21.5	22.2
32	894.3	146.6	25.3	21.3
33	916.0	104.5	22.3	20.8
34	940.0	133.4	28.0	20.1
35	963.3	158.3	20.8	21.9
36	985.8	156.8	24.9	21.7
37	1011.5	142.6	20.9	22.5
38	1039.0	145.8	22.3	21.9
39	1066.1	135.9	16.2	27.0
40	1094.4	132.6	18.1	28.3
41	1122.6	125.9	26.7	24.8
42	1150.9	128.3	27.7	25.2
43	1176.5	130.8	20.7	26.0
44	1199.5	127.7	22.6	25.4
45	1222.5	131.3	24.5	26.2
46	1250.0	142.6	25.0	22.7
47	1276.3	142.7	21.2	21.0

48	1296.8	142.8	25.4	21.0
49	1321.5	133.5	23.8	22.8
50	1352.5	144.8	21.9	25.1
51	1378.5	144.9	18.1	25.5
52	1399.5	136.1	21.0	24.8
53	1422.5	133.4	21.3	21.2
54	1446.2	132.5	21.2	25.3
55	1470.5	134.4	20.9	26.0
56	1494.8	127.1	25.6	23.1
57	1525.1	160.0	17.4	24.7
58	1561.4	153.0	22.7	33.2
59	1597.6	153.9	24.4	34.3
60	1633.9	142.0	26.6	27.2
61	1677.6	158.4	16.8	36.0
62	1728.9	157.9	18.0	24.0
63	1780.1	154.6	19.6	29.3
64	1831.4	152.0	24.5	28.7
65	1866.8	141.6	22.7	25.2
66	1886.5	142.3	22.0	21.8
67	1906.2	145.1	26.2	21.8
68	1929.0	149.7	28.7	9.8
69	1952.5	185.4	20.2	17.0
70	1973.5	180.4	23.7	20.0
71	1995.5	175.7	24.8	17.6
72	2018.5	137.2	27.7	18.6
73	2044.8	198.5	22.6	18.8
74	2074.3	200.8	24.7	20.4
75	2102.5	176.3	22.6	13.0
76	2129.5	170.9	25.2	16.7
77	2156.8	172.5	12.3	25.9
78	2184.3	171.8	22.8	24.0
79	2206.0	N.A.	N.A.	N.A.
80	2233.0	137.8	22.2	32.3
81	2263.8	170.3	21.7	35.0
82	2287.5	175.8	23.8	36.4
83	2311.2	176.0	22.7	33.4
84	2335.5	172.5	21.8	41.6
85	2360.5	179.4	20.4	44.3
86	2385.5	170.8	24.7	34.3
87	2415.0	174.6	22.0	17.0
88	2444.3	167.8	22.6	14.8
89	2468.8	166.2	26.0	15.1
90	2495.4	156.4	23.9	17.1
91	2524.1	153.0	23.0	14.5
92	2552.9	149.4	26.6	14.4
93	2581.6	149.7	28.1	19.4
94	2608.2	174.2	27.0	20.6
95	2632.5	174.6	25.1	20.2
96	2656.8	172.8	27.2	24.1
97	2682.2	148.9	28.9	21.3
98	2708.5	155.8	24.8	19.7
99	2734.8	150.1	27.2	22.3
100	2766.5	179.3	30.4	17.4
101	2798.2	180.9	24.6	37.1
102	2824.5	177.6	22.5	20.3
103	2850.8	179.1	28.0	28.2
104	2884.5	132.4	33.5	23.8
105	2922.8	176.7	19.3	24.5
106	2958.3	173.7	20.5	23.2

107	2993.8	174.8	25.4	15.4
108	3029.3	173.3	29.8	15.4
109	3058.8	122.7	27.5	29.7
110	3082.5	125.9	25.6	29.4
111	3106.2	128.7	18.3	25.9
112	3129.8	129.1	20.4	38.5
113	3153.5	122.8	25.6	36.2
114	3177.2	119.0	20.9	33.4
115	3201.3	162.2	24.8	30.9
116	3226.0	159.1	25.2	31.8
117	3250.7	151.0	22.6	37.0
118	3275.3	147.2	29.0	39.9
119	3300.0	151.4	29.6	30.6
120	3324.7	146.3	27.7	35.0
121	3355.5	162.4	29.9	22.5
122	3392.5	171.1	23.1	17.7
123	3425.8	155.6	30.1	33.3
124	3455.3	163.1	31.3	33.3
125	3484.8	159.7	26.6	22.6
126	3514.3	157.8	27.6	29.2
127	3542.0	152.9	25.9	27.7
128	3575.0	170.3	26.9	27.0
129	3607.3	182.2	26.8	19.0
130	3631.8	181.3	26.1	19.8
131	3666.0	173.5	29.8	22.9
132	3702.5	166.1	24.8	22.1
133	3730.5	181.9	27.8	28.9
134	3758.5	174.7	27.3	22.7
135	3789.0	173.4	31.5	24.9
136	3819.5	183.2	29.1	22.0
137	3856.0	182.5	28.3	26.0
138	3896.0	164.8	32.6	27.5
139	3923.5	156.4	26.7	26.2
140	3947.5	191.8	30.4	28.8
141	3982.5	201.6	29.4	28.7
142	4017.0	146.3	27.7	26.0
143	4047.5	162.0	29.6	28.5
144	4080.5	163.8	24.4	36.1
145	4107.5	140.5	22.4	30.0
146	4134.0	161.5	33.7	51.0
147	4163.3	146.4	25.2	40.1
148	4190.0	145.0	25.1	35.2
149	4216.7	148.3	28.6	38.1
150	4245.0	158.7	26.2	49.3
151	4281.0	171.7	30.2	32.2
152	4312.3	157.3	29.9	29.5
153	4332.8	147.1	32.6	29.5
154	4360.5	149.4	28.9	29.8
155	4392.5	141.1	33.1	35.0
156	4421.0	151.3	28.2	34.0

ChRM: Characteristic Remanent Magnetization; N.A.: data not available.

**Table DR2** –Paleomagnetic and bulk susceptibility ( $K_z$ ) measurements of Permo-Carboniferous rhythmites from Trombudo Central (RS rhythmites), state of Santa Catarina, S. Brazil (49.58°W 27.17°S). From Franco (2007).

Site		Direction of ChRM		Bulk Susceptibility
Stratigraphic Position	Relative Height (mm)	Declination (°E)	Inclination (°)	$K_z$ ( $10^{-5}$ CGS)
1	11.5	166.2	47.9	11.3
2	34.5	169.8	53.3	11.4
3	57.5	162.0	53.6	13.0
4	82.3	166.9	45.9	14.2
5	108.8	159.8	50.1	13.8
6	135.5	169.5	39.1	12.9
7	162.5	143.3	63.6	16.0
8	188.0	161.6	43.7	13.7
9	212.0	181.4	61.6	16.8
10	N.A.	N.A.	N.A.	N.A.
11	278.5	136.8	71.2	23.9
12	299.3	157.9	42.1	13.0
13	317.8	139.8	65.3	21.0
14	339.5	155.0	66.9	22.6
15	N.A.	N.A.	N.A.	N.A.
16	N.A.	N.A.	N.A.	N.A.
17	N.A.	N.A.	N.A.	N.A.
18	439.0	146.0	70.7	21.1
19	472.0	193.9	64.8	19.4
20	508.0	164.9	65.3	17.1
21	539.0	161.2	69.6	22.2
22	N.A.	N.A.	N.A.	N.A.
23	588.5	178.4	69.9	18.5
24	611.5	162.7	65.1	18.9
25	634.0	170.8	50.3	22.5
26	657.5	171.9	59.6	18.0
27	N.A.	N.A.	N.A.	N.A.
28	715.0	170.7	63.4	21.6
29	754.5	165.7	64.2	18.4
30	801.0	160.7	68.2	15.4
31	836.2	159.4	58.1	13.0
32	860.5	169.2	58.7	11.9
33	884.8	152.4	59.4	12.6
34	907.5	156.6	42.1	12.4
35	928.5	157.3	65.2	13.3
36	949.5	141.1	57.6	11.1
37	972.5	165.6	59.6	13.2
38	997.5	157.2	54.4	10.2
39	1022.5	160.7	56.5	12.6
40	N.A.	N.A.	N.A.	N.A.
41	N.A.	N.A.	N.A.	N.A.
42	N.A.	N.A.	N.A.	N.A.
43	N.A.	N.A.	N.A.	N.A.
44	1305.5	161.7	41.2	12.5
45	1334.5	169.1	65.4	15.5
46	N.A.	N.A.	N.A.	N.A.
47	N.A.	N.A.	N.A.	N.A.
48	N.A.	N.A.	N.A.	N.A.
49	1495.0	127.2	59.3	18.9
50	1524.3	136.6	77.0	14.2
51	1546.8	188.6	60.0	16.8

52	N.A.	N.A.	N.A.	N.A.
53	N.A.	N.A.	N.A.	N.A.
54	1620.0	217.5	61.9	14.0
55	1640.0	212.4	71.8	13.6
56	1662.0	160.7	59.6	16.5
57	1686.0	156.9	51.5	16.2
58	1711.8	149.9	54.4	15.2
59	1739.3	170.8	63.4	13.7
60	1765.5	165.8	53.8	16.7
61	1790.5	159.7	59.2	12.6
62	1817.3	147.2	69.1	11.8
63	1845.8	154.9	60.2	11.2
64	1870.5	100.6	54.7	12.5
65	1891.5	91.3	63.1	11.4
66	1912.5	111.5	58.7	10.4
67	1933.5	110.3	54.8	11.2
68	1956.8	162.6	49.0	10.9
69	1982.3	156.1	63.4	11.8
70	N.A.	N.A.	N.A.	N.A.
71	2060.0	164.3	61.1	16.6
72	2092.0	153.7	53.6	11.3
73	2121.3	161.8	59.3	13.3
74	2147.8	160.8	57.8	12.0
75	N.A.	N.A.	N.A.	N.A.
76	N.A.	N.A.	N.A.	N.A.
77	2254.5	159.7	54.4	5.3
78	2273.5	150.3	72.9	20.1
79	N.A.	N.A.	N.A.	N.A.
80	N.A.	N.A.	N.A.	N.A.
81	2349.5	150.6	67.0	19.9
82	N.A.	N.A.	N.A.	N.A.
83	2403.5	321.6	58.6	17.1
84	2430.0	155.4	66.8	22.4
85	2454.0	133.5	66.0	17.1
86	2480.5	139.5	54.9	21.5
87	2504.0	145.7	50.8	15.6
88	2526.0	149.1	58.2	12.7
89	N.A.	N.A.	N.A.	N.A.
90	N.A.	N.A.	N.A.	N.A.
91	2627.0	160.9	58.4	16.0
92	2647.0	157.4	59.1	8.8
93	2667.0	162.4	57.0	14.6
94	2686.0	155.9	47.3	14.2
95	2704.0	152.1	62.0	16.6
96	N.A.	N.A.	N.A.	N.A.
97	2752.0	150.5	42.6	11.0
98	2772.0	167.5	64.9	17.4
99	2802.5	246.2	58.9	16.6
100	N.A.	N.A.	N.A.	N.A.
101	N.A.	N.A.	N.A.	N.A.
102	2881.0	163.7	61.2	15.7
103	2910.0	140.5	62.1	21.9
104	N.A.	N.A.	N.A.	N.A.
105	2969.3	342.2	52.8	15.3
106	2990.0	351.9	56.1	14.8
107	3010.7	338.1	59.6	14.1
108	N.A.	N.A.	N.A.	N.A.
109	3095.3	156.9	59.0	14.9
110	3124.0	169.0	46.4	8.1

111	3152.7	158.6	54.6	12.4
112	3179.2	156.3	60.1	19.2
113	3203.5	152.4	56.8	13.4
114	3227.8	159.3	61.0	14.7
115	3252.0	156.8	66.9	17.7
116	3276.0	164.5	56.1	10.3
117	3300.0	150.2	54.0	13.1
118	3322.0	163.3	54.4	14.8
119	3342.0	158.0	60.8	16.6
120	3363.3	333.4	44.7	12.4
121	3385.8	343.7	50.0	19.1
122	3409.5	142.2	65.6	22.1
123	3430.3	163.2	52.4	16.0
124	3446.8	165.4	50.1	21.9
125	N.A.	N.A.	N.A.	N.A.
126	N.A.	N.A.	N.A.	N.A.
127	3516.0	157.3	45.9	16.4
128	3536.0	152.9	65.9	16.6
129	N.A.	N.A.	N.A.	N.A.
130	3669.2	162.2	49.8	17.4
131	3689.6	147.1	51.6	8.9
132	3710.0	158.2	58.2	11.3
133	3730.4	153.7	54.6	11.0
134	3750.8	158.1	48.8	16.0
135	3773.0	147.2	55.8	14.7
136	3797.0	154.3	53.4	11.1
137	3821.0	153.2	56.8	13.3
138	3846.0	154.7	60.7	14.4
139	3872.0	153.9	50.9	10.9
140	3898.0	154.6	48.2	14.7
141	3923.8	140.9	56.5	13.7
142	3949.5	149.3	56.6	13.5
143	3975.2	157.3	56.2	12.6
144	N.A.	N.A.	N.A.	N.A.
145	4086.6	171.1	57.3	11.0
146	4117.9	169.6	61.6	10.9
147	4149.1	169.5	63.0	9.9
148	4180.4	148	47.3	10.7
149	4210.0	142.3	58.3	11.8
150	4238.0	141.1	59.4	11.2
151	4266.0	137	58.6	11.7
152	4294.0	147.7	59.4	10.9
153	4322.0	146.7	56.1	13.0
154	4353.0	133.5	63.5	11.5
155	4387.0	142.5	64.8	10.6
156	4421.0	153.6	45.6	8.2
157	4455.0	156.3	51.0	10.1

ChRM: Characteristic Remanent Magnetization; N.A.: data not available.

## D. Low frequency spectra

The series from both localities present special challenges for spectrum evaluation, particularly in the lowest frequency bands, due to their short lengths relative to some of the most important frequencies of interest (Milankovitch frequencies). The insets shown in Fig. 3A,B present results for single and multiple harmonic line tests; these tests are not fail-safe, and can indicate apparent lines from random variations (Schulz and Stategger, 1997). Testing with red noise models

reduces the possibility of such “false alarms.” Fig. DR5 shows results of robust red noise modeling and multitapered power spectra of interpolated, zero-padded versions of the K<sub>z</sub> series from both localities. The noise models are biased due to the interpolation, but this tends to elevate noise spectral estimates at the lowest frequencies. The spectral peaks exceeding the 95% confidence limits are labeled, and may be compared to the harmonic tests in Fig. 3 A,B.

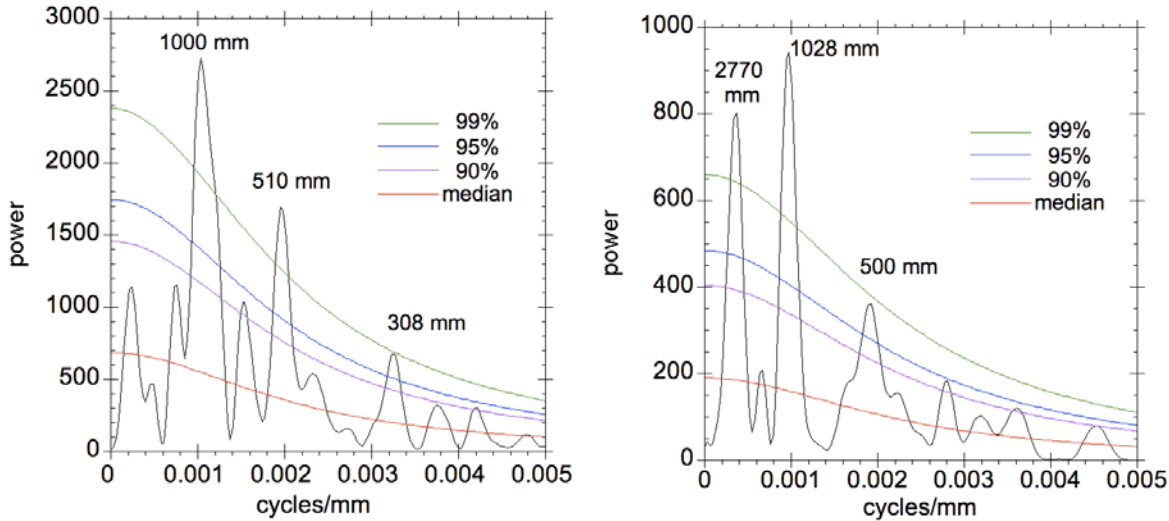


**Figure DR5.** Robust red noise study of (A) the Itu (IT) K<sub>z</sub> series and (B) the Rio do Sul (RS) K<sub>z</sub> series using the SSA-MTM-toolkit with three  $2\pi$  prolate tapers (Ghil et al., 2002). The red noise was modeled using a linear fit and a median filter band of 0.001 cycles/mm. Both K<sub>z</sub> series were preprocessed by interpolating to  $\Delta d=1.0$  mm, and zero-padded to 5 times the original series length. The original sample spacing of the IT series was  $28.4 \pm 5.5$  mm (see Fig. 2A, Curve 4); the original sample spacing was  $35.8 \pm 32.8$  mm (see also Fig. 2B, Curve 4). The black curve is the estimated power spectrum of the K<sub>z</sub> series; the other curves indicate the robust red noise model (red curve), and the 90%, 95% and 99% confidence limits.

## E. References

- Archanjo, C.J., Silva, M.G., Castro, J.C., Launeau, P., Trindade, R.I.F., and Macedo, J.W.P., 2006, AMS and grain shape fabric of the Late Palaeozoic diamictites of the Southeastern Paraná Basin, Brazil: Journal of the Geological Society, v. 163, p. 95-106.
- Canuto, J.R., 1993. Fácies e Ambientes de Sedimentação da Formação Rio do Sul (Permiano), Bacia do Paraná, na Região de Rio do Sul, Estado de Santa Catarina [Ph.D. thesis]: University of São Paulo, 164 p.
- Eyles, C.H., Eyles, N., and França, A.B., 1993, Glaciation and tectonics in an intracratonic basin: the Late Palaeozoic Itararé Group, Paraná Basin, Brazil: Sedimentology, v. 40, p. 1-25.
- França, A.B., and Potter, P.E., 1991, Stratigraphy and reservoir potential of glacial deposits of the Itararé group (Carboniferous-Permian), Paraná Basin, Brazil: Association of Petroleum Geologists Bulletin, v. 75, p. 62-85.

Franco, D.R., 2007, Magnetoestratigrafia e Análise Espectral de Ritmitos Permocarboníferos da Bacia do Paraná: Influências dos Ciclos Orbitais no Regime Depositional [Ph.D. thesis]: Universidade de São Paulo, 192 p.

Franco, D.R., Hinnov, L.A., and Ernesto, M., Spectral analysis and modeling of microcyclostratigraphy in Late Paleozoic glaciogenic rhythmites (Paraná Basin, Brazil): Geochemistry, Geophysics, Geosystems, doi:10.1029/2011GC003602, in press.

Ghil, M., Allen, R.M., Dettinger, M.D., Ide, K., Kondrashov, D., Mann, M.E., Robertson, A., Saunders, A., Tian, Y., Varadi, F., and Yiou, P., 2002, Advanced spectral methods for climatic time series: Reviews of Geophysics, v. 40, 1003, doi: 10.1029/2000RG000092.

Rocha-Campos, A.C., 1967, The Tubarão Group in the Brazilian portion of the Paraná Basin: in Bigarella, J.J., Becker, R.D., Pinto, I.D. (Eds.), Problems in Brazilian Gondwana Geology, UFPR, Curitiba, p. 27-102.

Rocha-Campos, A.C., Ernesto, M., and Sundaram, D., 1981, Geological, palynological and paleomagnetic investigations on Late Paleozoic varvites from the Paraná Basin, Brazil: in *Simpósio Regional de Geologia, Acta*, v. 3, p. 162-175.

Rocha-Campos, A.C., 2000, Varvite from Itu, São Paulo state, in *Sítios Geológicos e Paleontológicos do Brasil*, eds. Schobbenhaus, C., Campos, D.A., Queiroz, E.T., Winge, M., & Berbert-Born, M. Published on Internet at the address <http://www.unb.br/ig/sigep/sitio062/sitio062.htm>.

Rocha-Campos, A.C., Canuto, J.R., and Santos, P.R., 2000, Late Paleozoic glaciotectonic structures in northern Paraná Basin, Brazil: Sedimentary Geology, v. 130, p. 131-143.

Santos, P.R., Rocha-Campos, A.C., and Canuto, J.R., 1992, Estruturas de arrasto de icebergs em ritmitos do Subgrupo Itararé (Neopaleozóico), Trombudo Central, SC: Boletim IGUSP, Série Científica, v. 23, p. 1-18.

Santos, P.R., Rocha-Campos, A.C., and Canuto, J.R., 1996, Patterns of Late Paleozoic deglaciation in the Paraná Basin, Brazil: Palaeogeography, Palaeoclimatology, Palaeoecology, v. 125, p. 165-184.

Schulz, M. and Stategger, K., 1997.

Sinito, A.M., Valencio, D.A., Ernesto, M., and Pacca, I.G., 1981. Palaeomagnetic study of Permocarboniferous glacial varves from the Itararé Subgroup, southern Brazil: Geophysical Journal of the Royal Astronomical Society, v. 67, p. 635-640.

Vesely, F.F., and Assine, M.L., 2002, Superfícies estriadas em arenitos do Grupo Itararé produzidas por gelo flutuante, sudeste do estado do Paraná: Revista Brasileira de Geociências, v. 32 (4), p. 587-594.